Real-time model predictive control of a wastewater treatment plant based on machine learning

A. Bernardelli, S. Marsili-Libelli, A. Manzini, S. Stancari, G. Tardini, D. Montanari, G. Anceschi, P. Gelli and S. Venier

ABSTRACT

Two separate goals should be jointly pursued in wastewater treatment: nutrient removal and energy conservation. An efficient controller performance should cope with process uncertainties, seasonal variations and process nonlinearities. This paper describes the design and testing of a model predictive controller (MPC) based on neuro-fuzzy techniques that is capable of estimating the main process variables and providing the right amount of aeration to achieve an efficient and economical operation. This algorithm has been field tested on a large-scale municipal wastewater treatment plant of about 500,000 PE, with encouraging results in terms of better effluent quality and energy savings.

Key words | Artificial Intelligence, machine learning, model predictive control, neuro-fuzzy computing, nutrient removal, real-time control

A. Bernardelli
A. Manzini
S. Stancari
G. Tardini
D. Montanari
G. Anceschi
EnergyWay srl
Via Sant'Orsola, 33,
41121 Modena,
Italy

S. Marsili-Libelli (corresponding author)
University of Florence,
Piazza di San Marco, 4,
50121 Firenze FI,
Italy
E-mail: *stefano.marsililibelli@unifi.it*

P. Gelli
S. Venier
Gruppo HERA SpA,
Viale Carlo Berti Pichat, 2/4,
40127 Bologna (BO),
Italy

HIGHLIGHTS

- Artificial Intelligence helps improve the energy efficiency of a wastewater treatment plant.
- Model predictive control produces a better effluent quality in a wastewater treatment plant.
- A neuro-fuzzy controller improves the reliability of a wastewater treatment plant.

NOMENCLATURE

Acronyms

AI	Artificial Intelligence
AIE	Artificial Intelligence Engine
ANFIS	Adaptive Neuro-Fuzzy Inference System
CC	Conventional Controller
DO	Dissolved Oxygen (mg/l)
DO_{sp}	Dissolved Oxygen set-point (mg/l)
EW	Energy Way
FL	Fuzzy Logic
GA	Genetic Algorithm
MPC	Model Predictive Control
N_{tot}	Total Nitrogen (mgN/l)
PID	Proportional-Integral Derivative controller, equivalent to CC
Q_{in}	Input recycle flowrate (m^3/s)
Q_r	Internal recycle rate (percentage of maximum)
Q_{ras}	External recycle rate (percentage of Q_{in})
Q_w	Waster rate (percentage of Q_{in})
U_a	Air flow rate (Nm^3/h)
WWTP	Waste Water Treatment Plant

Symbols

NH_4^+	Ammonium-N concentration (mgN/l)
NO_3^-	Nitrate-N concentration (mgN/l)
NO_2^-	Nitrite-N concentration (mgN/l)
$\gamma_1, \gamma_2, \gamma_3$	Unconstrained optimisation coefficients
ρ_1, ρ_2, ρ_3	Constrained optimisation coefficients
δ	Control sampling time (min)
α, β	Prediction and control horizons, as multiples of δ

doi: 10.2166/wst.2020.298

INTRODUCTION

A wastewater treatment plant (WWTP) is a complex process that uses microbiological reactions to remove pollutants from wastewater. In its operation, this energy-intensive process must reconcile two partially conflicting objectives: pollution abatement and energy conservation. It appears that a balance between these two diverging goals can be achieved through automatic control based on Artificial Intelligence (AI).

In the last two decades, as recently documented, there has been a growing integration between Artificial Intelligence and wastewater treatment processes (Mannina *et al.* 2019; Zhao *et al.* 2020). Biological treatment processes are intrinsically complex, involving a variety of microbial communities, of natural conditions, of influent characteristics, each with inherent uncertainties and time changes. On the other hand, governing legislation demands consistent effluent standards, while financial constraints call for energy savings. Reconciling effluent quality and economical operation, given the time-varying and uncertain nature of the process, requires advanced control solutions, which can be provided by Artificial Intelligence. This powerful tool can cater for both of the process operational requirements previously defined.

Artificial Intelligence is a universe of differing mathematical tools, which can be roughly grouped into Artificial Neural Networks (Kosko, 1992; Hagan *et al.* 1996), Fuzzy Logic (Yager & Zadeh 1994; Babuska 1998), and Genetic Algorithms (Goldberg 1989; Holland 1998), each with varied sub-categories, as aptly analysed in Zhao *et al.* (2020). Often these techniques are combined to produce high-level supervisory systems, generally referred to as Expert Systems (Castillo *et al.* 2016; Torregrossa *et al.* 2018; Judson 2019; Nikolopoulos 2019) or Decision Support Systems specifically aimed at harmonising conflicting objectives in the design of WWTP (Iglesias *et al.* 2007; Snip *et al.* 2014; Corominas *et al.* 2018), as later reviewed by Mannina *et al.* (2019). AI tools have also been used in WWTP to develop soft sensors to provide a double-check, or even substitute for hard sensors (Haimi *et al.* 2013, 2016; Mulas *et al.* 2015; Fernandez de Canete *et al.* 2016).

The application of Artificial Intelligence to the wastewater treatment area has been documented in many successful applications. Unlike many industrial processes where an approximating linear model can be used to implement a model predictive controller (MPC) (Borrelli *et al.* 2017; Rawlings *et al.* 2017), WWTP is a highly nonlinear, time-varying process and ad-hoc versions of MPC must be designed. A carbon-dosing system based on a fuzzy model predictive controller was proposed by Marsili-Libelli & Giunti (2002) to improve the nitrification performance. An evolutionary self-organising model of a municipal WWTP based on genetic programming was designed by Hong & Bhamidimarri (2003) to successfully model the many process nonlinearities. The primary aspect of WWTP management is the harmonisation of the effluent quality requirements with the energy conservation. This challenge has produced many studies in which the multi-objective nature of the problem was approached with AI tools and solved by the application of MPC, resulting in a multi-loop structure, as surveyed by Qiao *et al.* (2018). Differing nitrogen control strategies were proposed by Stare *et al.* (2007), while the specific problem of dissolved oxygen (DO) control using an MPC was considered by Holenda *et al.* (2008). O'Brien *et al.* (2011) used an MPC to reduce the plant power consumption by a quarter. A multivariable MPC for improving the nitrogen removal and reducing the operational costs was proposed by Dainotto *et al.* (2012) and Mulas *et al.* (2013), to be later extended to the control of a full-scale WWTP (Han & Qiao 2014; Mulas *et al.* 2015; Foscoliano *et al.* 2016). Francisco *et al.* (2015) described a procedure to determine the most economically viable controlled variable in the WWTP and proposed a nonlinear MPC integrated with a PI to monitor the process constraints. A similar approach was used by Goldar *et al.* (2016) to design a decentralised nonlinear MPC combined with a PI controller, which compared favourably to the previous centralised controller based on PI alone.

MATERIAL AND METHODS

Description of the plant and the information technology

The WWTP from which the data were acquired, and which is being used as a test plant, is the municipal plant of the city of Modena, in Northern Italy. It consists of a conventional biological treatment plant for nutrient removal with predenitrification, with a capacity of approximately 500,000 PE.

The process instrumentation consists of a Dissolved Oxygen meter and a nutrient sensor (Hach, Endress + Hauser). These field measurements are routed to the plant SCADA for real-time operation. An encrypted connection between the plant and the Energy Way centre was created to allow prototypical testing. This arrangement enables specific clients to access the controller through a LAN. Through VPN encrypted tunnelling, clients can mount directories on the controller as NFS folders and obtain

services directly from the controller, enabling fast analysis iteration and maintenance.

Communication between the centre and the plant SCADA is based on the Modbus protocol over TCP/IP, physically linking the controlling machine to the PLC-front-end with an Ethernet patch cable, enabling peer-to-peer IP communication.

The AI components of the MPC were trained and validated using plant data spanning over one year of operation of the same plant.

Before this MPC was designed, the plant automation consisted of conventional Proportional-Integral-Derivative (PID) control loops, which are now used as yardsticks to assess the performance of the new controller.

ANFIS – a systematic approach to neuro-fuzzy modelling

The AIE applied in this study is based on an Artificial Neuro-Fuzzy Inference System (ANFIS). This structure, shown in Figure 1, was originally proposed by Jang (1993) and was later used, among other applications, to model wastewater treatment processes (Tay & Zhang 1999, 2000), drinking water processes (Wu *et al.* 2014), composting (Giusti & Marsili-Libelli 2010), irrigation management (Giusti & Marsili-Libelli 2015), flood forecasting (Bartoletti *et al.* 2018) and in the context of soft-sensors development (Dürrenmatt & Gujer 2011; Haimi *et al.* 2013). ANFIS, which is thoroughly described in Marsili-Libelli (2016), is a composite neuro-fuzzy structure that implements Sugeno-type fuzzy logic (Takagi & Sugeno 1985)

$$R_i: \textit{if } (x_1 \textit{ is } A_1^{(i)}) \ \ldots \textit{and} \ldots \ (x_n \textit{ is } A_n^{(i)}) \textit{ then } f_i = \mathbf{a}_i^T \cdot \mathbf{x} + b_i \tag{1}$$

where ($\mathbf{x} \in R^n$) is the vector of inputs, and ($\mathbf{a}_i$, b_i) are the coefficients of the linear Sugeno consequents.

The improvement of ANFIS with respect to the classical Sugeno fuzzy models is in its ability to adjust *both* the antecedent membership functions *and* the linear consequents to minimise the sum of squared differences between the ANFIS output and a training data set. As explained later, this structure has been used repeatedly to develop the MPC.

Development of the model predictive controller

The present real-time MPC was designed to improve the energy efficiency of the nutrient removal process in the full-scale municipal WWTP described earlier. The process control scheme is shown in Figure 2, where the set-points for the dissolved oxygen DO_{sp} and the recycle flow $Q_{r,sp}$ are determined on the basis of the forecasted future nutrient loading provided by the artificial intelligence engine (AIE). These set-points are fed to local controllers to deliver the proper amount of air flow (U_a) and internal recycle (Q_r). The grey boxes indicate the low-lever controllers/actuators.

The observed variables used to train the ANFIS are the DO, oxidation reduction potential (ORP), temperature, the nitrogen species (NH_4 and NO_3) in the oxidation tank, and the output total nitrogen (N_{tot}). The manipulated variables are the airflow rate (U_a) and the internal recycle Q_r, the latter expressed as a percentage (0–100%) of the maximal allowable flow. This reflects the fact that the recycle pump operates at a fixed regime, so the percentage represents the fraction of the ON time in each time frame.

It is assumed that the controlled variables (DO and Q_r) can track their set-points without appreciable error, being

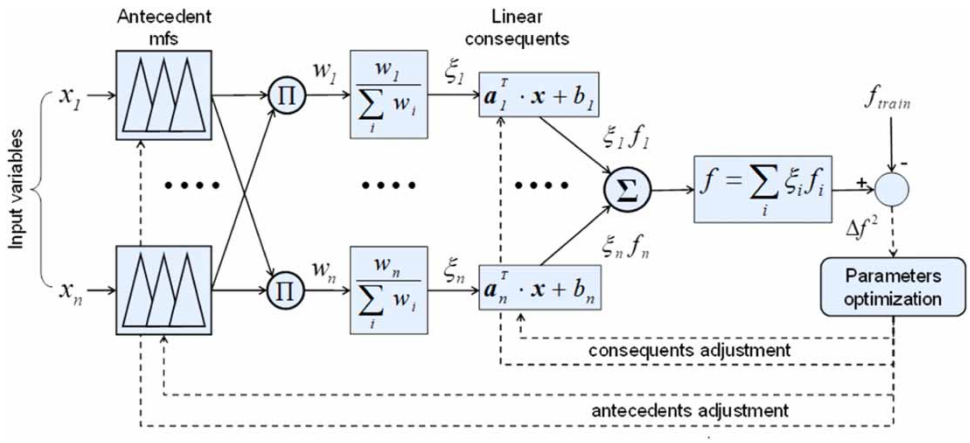

Figure 1 | General structure of ANFIS. The dashed lines indicate the adjustment paths of both the antecedents and the consequents, depending on the squared error between the ANFIS output and the training data (Marsili-Libelli 2016).

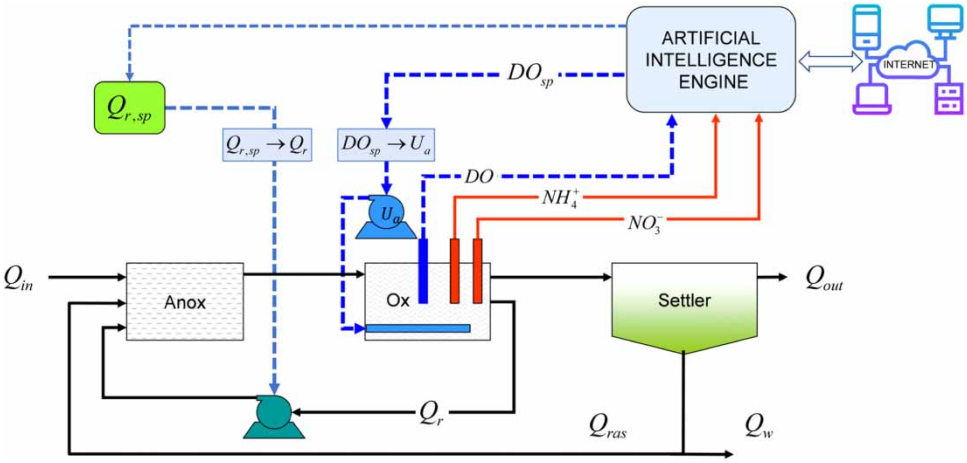

Figure 2 | Process scheme of the WWTP to which the MPC is applied. The two control loops are indicated by the dashed lines: the DO control loop regulates the airflow (U_a), while the recycle loop controls the internal recycle (Q_r).

locally controlled by low-level PID regulators. They act on the blowers delivering the air flow U_a and on the recycle pump providing the internal recycle (Q_r). The MPC aims to reduce the amount of output total nitrogen (N_{tot}), while at the same time minimising the energy consumption.

All of the process variables are sampled at regular intervals $\delta = 5$ min, which represents the MPC time-base, of which the control (β) and prediction (α) horizons are multiples. The control horizon is equal to the sampling time, so $\beta = 1$, while the prediction horizon $\alpha > \beta$ was suitably defined as a multiple of β, which cannot be further specified here because of industrial confidentiality.

The purpose of the MPC is the minimisation of the following performance function, which takes into account both the predicted nitrogen species and the energy consumption, represented by the blower energy consumption E.

$$DO^*_{sp}(t+\beta) = \underset{DO_{sp}}{arg\min} \left[\begin{array}{l} \gamma_1 \dfrac{\hat{NH}_4^+(t+\alpha) + \hat{NO}_3(t+\alpha)}{\overline{N_{tot}}} + \gamma_2 \dfrac{E(t+\beta)}{\bar{E}} + \\ \gamma_3 \dfrac{DO_{sp}(t+\beta) - DO_{sp}(t)}{\overline{DO_{sp}}} + \rho_1 \dfrac{\hat{NH}_4(t+\alpha)}{\overline{NH_4}} + \\ \rho_2 \dfrac{\hat{NO}_3(t+\alpha)}{\overline{NO_3}} + \rho_3 \dfrac{\hat{N}_{tot}(t+\alpha)}{\overline{N_{tot}}} \end{array} \right]$$

$$where\ N_{tot} = NH_4^+ + NO_3^-$$

$$\gamma_1, \gamma_2, \gamma_3, \rho_1, \rho_2, \rho_3 = weighting\ factors;$$

$$E = blower\ energy$$

$$\bar{\cdot} = average\ value;\ \alpha = \text{prediction horizon};$$

$$\beta = \text{control horizon}. \qquad (2)$$

While the γ weights are always active, the ρ coefficients can be regarded as 'soft constraints' because they are activated whenever each variable reaches its upper bound

$$\begin{aligned} &\rho_1 \neq 0 \ \ if \ \ \hat{NH}_4(t+\alpha) \geq NH_4^* \\ &\rho_2 \neq 0 \ \ if \ \ \hat{NO}_3(t+\alpha) \geq NO_3^* \\ &\rho_3 \neq 0 \ \ if \ \ \hat{N}_{tot}(t+\alpha) \geq N_{tot}^* \end{aligned} \qquad (3)$$

with NH_4^*, NO_3^*, N_{tot}^* fixed threshold values.

The following feedforward control generates the next recycle flowrate $Q_r(t+\beta)$ by updating the current value $Q_r(t)$ according to the forecasted NO_3 value

$$\hat{Q}_r(t+\beta) = Q_r(t) + \frac{\hat{NO}_3^-(t+\alpha) - \hat{NO}_3^-(t)}{\hat{NO}_3^-(t)} \qquad (4)$$

Then $\hat{Q}_r(t+\beta)$ is constrained between 60% and 100% of the allowable range, namely

$$Q_r(t+\beta) = \begin{cases} \min(\hat{Q}_r(t+\beta), 100) \\ \max(60, \hat{Q}_r(t+\beta)) \end{cases} \qquad (5)$$

Equation (4) indicates that for operational reasons the internal recycle must remain inside the range [60, 100]% of its nominal value, in other terms it can only be decreased down to nearly half its nominal value, but not increased beyond that limit. The inner structure of the MPC is shown in Figure 3, and consists of two parts

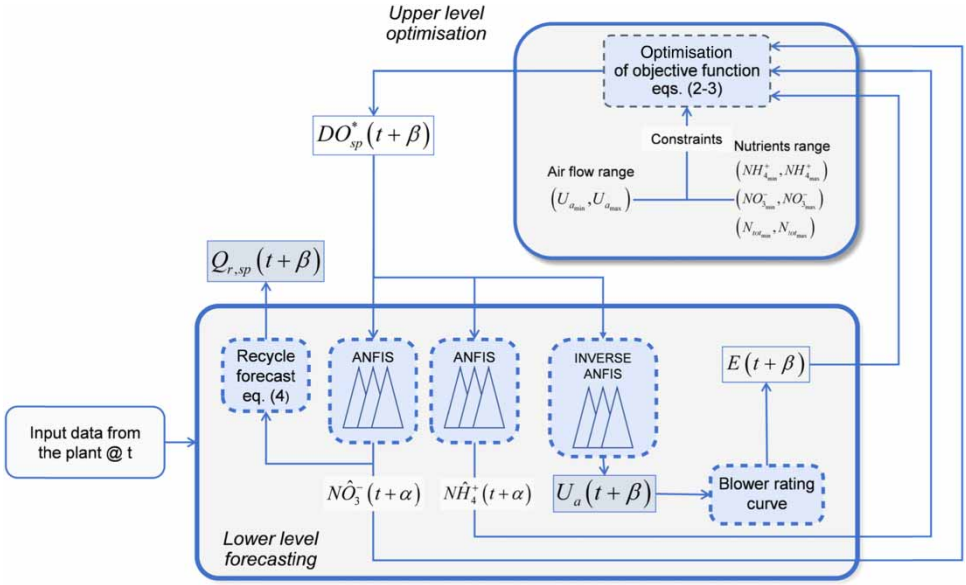

Figure 3 | General scheme of the neuro-fuzzy MPC. The prediction is made α steps ahead, while the control is applied at β steps ahead. The grey boxes represent the manipulated variables to be applied to the plant at the next step ($t+\beta$).

represented by the dashed boxes: the optimisation in the upper block implements Equations (2) and (3), while the lower block produces the forecasts on which the optimisation is based. The purpose of the upper block is to determine the best DO_{sp} by testing all of the possible $DO_{sp}(t+\beta)$ values, within a predefined grid of values, on the basis of the forecasts of the lower block. The current $DO_{sp}(t+\beta)$ under test is also fed into the inverse ANFIS, which yields the corresponding value of air flow $U_a(t+\beta)$. From the blower rating curve, this value is converted into the energy consumption $E(t+\beta)$, which is returned to the upper block. The lower block also computes the next recycle flow $Q_r(t+\beta)$ according to Equations (4) and (5).

The prediction accuracy is assessed through the following performance indexes computed over n samples:

$$MAE\ (Mean\ Absolute\ Error) = \frac{1}{n}\sum_{i=1}^{n}|\hat{y}_i - y_i|$$
$$RAE\ (Relative\ Absolute\ Error) = 100 \times \frac{1}{n}\sum_{i=1}^{n}\left|\frac{\hat{y}_i - y_i}{y_i}\right|, \quad (6)$$

where y represents the actual generic variable and $\hat{y}$ its estimate. Figure 4 shows the performance of the trained neuro-fuzzy predictors in estimating the process variables α steps ahead for the nitrogen species and β steps ahead for the airflow.

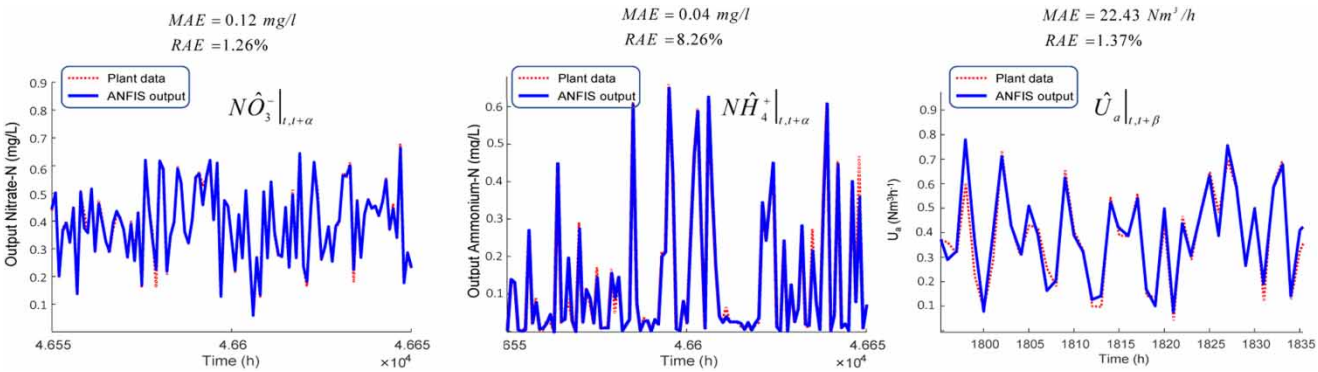

Figure 4 | Performance of process variables prediction, at time $t+\alpha$ for the nutrients and at $t+\beta$ for the airflow provided by the trained neuro-fuzzy networks. Normalised values are shown to preserve confidentiality.

A sensitivity assessment was also performed on the model by considering the percentage variations of the output variables (NH_4^+, NO_3^-) caused by a ±20% variation in DO. Figure 5(a) shows that a positive DO variation of 20% produces a NH_4^+ decrease in 95.8% of the cases (red bars), while a −20% DO variation results in an increase of NH_4^+ in 96.1% of the times (blue bars). Likewise, Figure 5(b) shows that a +20% DO increase is followed by an NO_3^- increase in 91.7% of the cases, while a −20% DO decrease results in a lower NO_3^- in 92.3% of the times. The spread in the response is due to the influence of other process conditions.

RESULTS AND DISCUSSION

After testing the consistency of the predictions via error assessment of Equation (6) and the sensitivity analysis, the proposed EW controller has been compared to the conventional controller (CC) that was previously in operation. The preliminary test shown in Figure 6 consists of three time-windows and compares the total output nitrogen (N_{tot}) produced by the two controllers, only one of which is engaged at any one time. The total output nitrogen follows the reference value produced by the active controller within the model error tolerance. In the first and third time-window, the conventional controller (CC) is active, yielding a higher value of N_{tot}, while in the central grey window, the EW controller is engaged and produces a lower output N_{tot}. However, since both controllers are always updated, they continue to produce a reference output even when disengaged. Hence, in the grey slot, the CC controller still produces a higher reference, which, however, has no effect on the output because it is disconnected, being disengaged.

A further test was then carried out to test the EW controller's adaptability to differing operational situations,

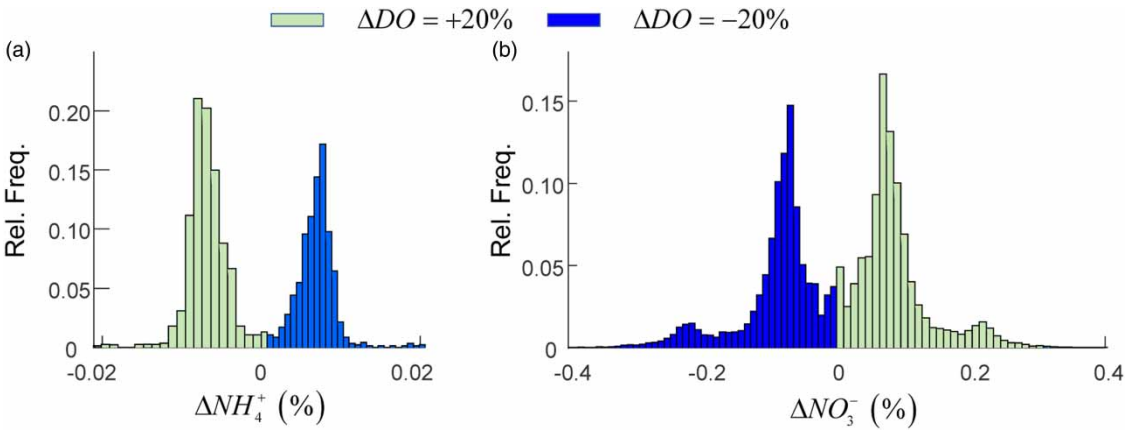

Figure 5 | Sensitivity assessment of the ANFIS predictors (lower block in Figure 3). The ammonium-N variations (ΔNH_4^+) in response to a 20% change in DO are shown in (a), while (b) shows the corresponding ΔNO_3^- variations. Note the opposite response of the two output variables. Please refer to the online version of this paper to see this figure in colour: http://dx.doi.org/10.2166/wst.2020.298.

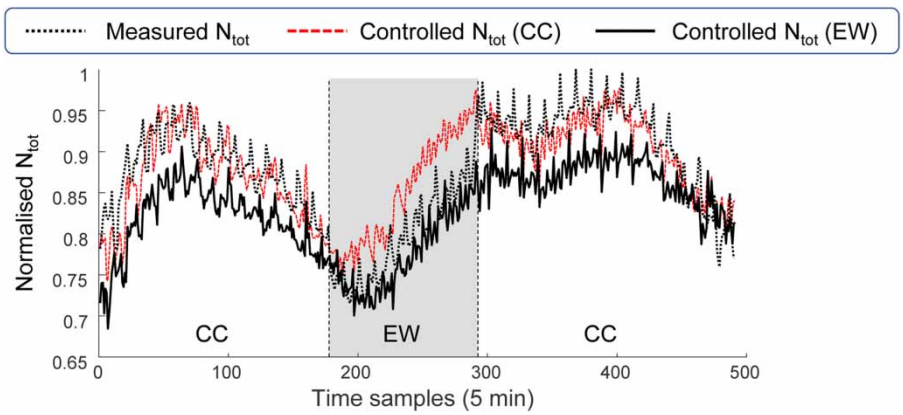

Figure 6 | Comparison of total-N output with the conventional (CC) and EW controller, operating between samples 180 and 280 (shaded area) corresponding to the test period in March 2019. A lower N_{tot} output was obtained by the EW controller.

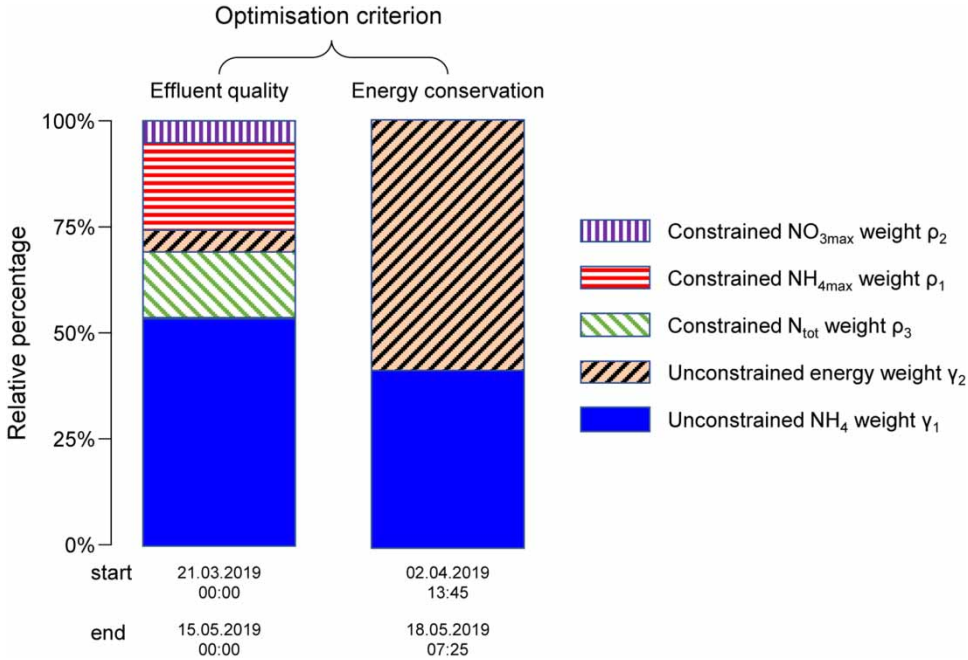

Figure 7 | Average relative weights in the performance function Equation (2) during two separate EW controller experiments in the period indicated below each bar. In the left bar, the emphasis is on effluent quality, and thus the most active constraint is on NH_4 and N_{tot}, while in the right bar the energy term γ_2 is the most important. Please refer to the online version of this paper to see this figure in colour: http://dx.doi.org/10.2166/wst.2020.298.

putting the emphasis either on the effluent quality, or on the energy conservation, as the conditions required. Figure 7 shows the average relative weights of the performance function Equations (2) and (3) during two different periods in which the EW controller was operating. The left bar corresponds to a high-load condition, when the effluent quality is the primary concern. The blue bar, corresponding to the unconstrained NH_4 term γ_1, is predominant because the premium is set on limiting the ammonium-N discharge. For the same reason, the constrained weight on N_{tot} (ρ_3) is the second largest coefficient, while the energy weight γ_2 is comparatively much smaller. The severity of the loading is also apparent in the comparatively large activation of the constrained terms ρ_1, ρ_2, and ρ_3, indicating that both Nitrogen species are approaching their limit.

The right bar, by contrast, shows the weights distribution during a mild load period, during which energy saving becomes the primary concern. It can be seen that while the constrained weights ρ_1, ρ_2, and ρ_3 are not activated, the energy weight γ_2 is now the dominant one.

This performance assessment shows that the EW controller is able to combine the two operational modes and selects the overall goal to be pursued, depending on the incoming load, by dynamically adapting its performance function Equations (2) and (3), depending on the present and predicted loading conditions.

After the goal-shifting experiments of Figure 7, the two controllers were run on alternate weeks from 10 June to 9 September 2019. To compare their performance over this period, the influent NH_4 was divided into three classes based on percentiles, as shown in Table 1, and the corresponding effluent NH_4 was observed.

Table 2 summarises the performance of the two controllers during this period. It shows that while the average input NH_4 is nearly the same for both controllers, indicating two comparable operational periods, their process management is very different: looking at the values of the DO_{sp} and actual DO value, they are both higher in the CC case, indicating a larger energy consumption. Conversely, the EW controller keeps the DO lower, but still at a safe level, to ensure adequate NH_4 oxidation. It is not surprising that the air flow is highest for both controllers in the Medium input range, because in this segment the oxidation

Table 1 | Partitioning of influent NH_4 during the period 10 June–9 Sept. 2019 into three classes

Influent NH_4 class	Percentile range	NH_4 values (mg/l)
Low	0–25th	0–17.9
Medium	25th–75th	17.9–28.7
High	75th–100th	28.7–62.8

Table 2 | Weekly averages of the main process variables over the period 10 June – 9 Sept. 2019

	Input NH_4		DO		DO_{sp}		Air flow		Output NO_3		Output NH_4		Output N_{tot}	
NH_4 class	**CC**	**EW**	**CC**	**EW**	**CC**	**EW**	**CC**	**EW**	**CC**	**EW**	**CC**	**EW**	**CC**	**EW**
Low	5.23	8.63	0.95	0.49	0.48	0.31	1,194.42	1,081.35	5.96	6.10	0.61	0.89	6.56	6.99
Medium	25.14	24.05	0.56	0.47	0.49	0.42	1,425.83	1,240.48	6.84	6.15	0.95	1.11	7.79	7.26
High	32.47	31.99	0.54	0.44	0.50	0.38	1,135.97	876.09	8.36	6.19	0.73	1.13	9.09	7.32

needs are highest, while in the High range of NH_4, the air flow can be safely decreased without exceeding the effluent allowable limit.

Table 3 | Performance improvement of EW over CC during the period 10 June – 9 Sept. 2019

	Measured averages over the three input classes			
	Effluent N_{tot}	**Air flow (U_a)**	**DO**	**Energy saving**
Δ(EW-CC) %	−8.1%	−16.7%	−29.0%	−16.0%

The EW controller achieves a better overall performance, though the output ammonium-N is higher, but still within the regulatory limit. This is due to the fact that the EW controller lowers the DO_{sp} in order to save energy and avoid an excessive nitrate-N build-up, which would then be difficult to eliminate in the denitrification phase because of the limited availability of organic carbon. In fact, although the ammonium-N output is slightly higher than that produced by the CC controller, it still remains well within the prescribed limit, so any further reduction in output NH_4 would only imply a larger energy expenditure, without any benefit in effluent quality.

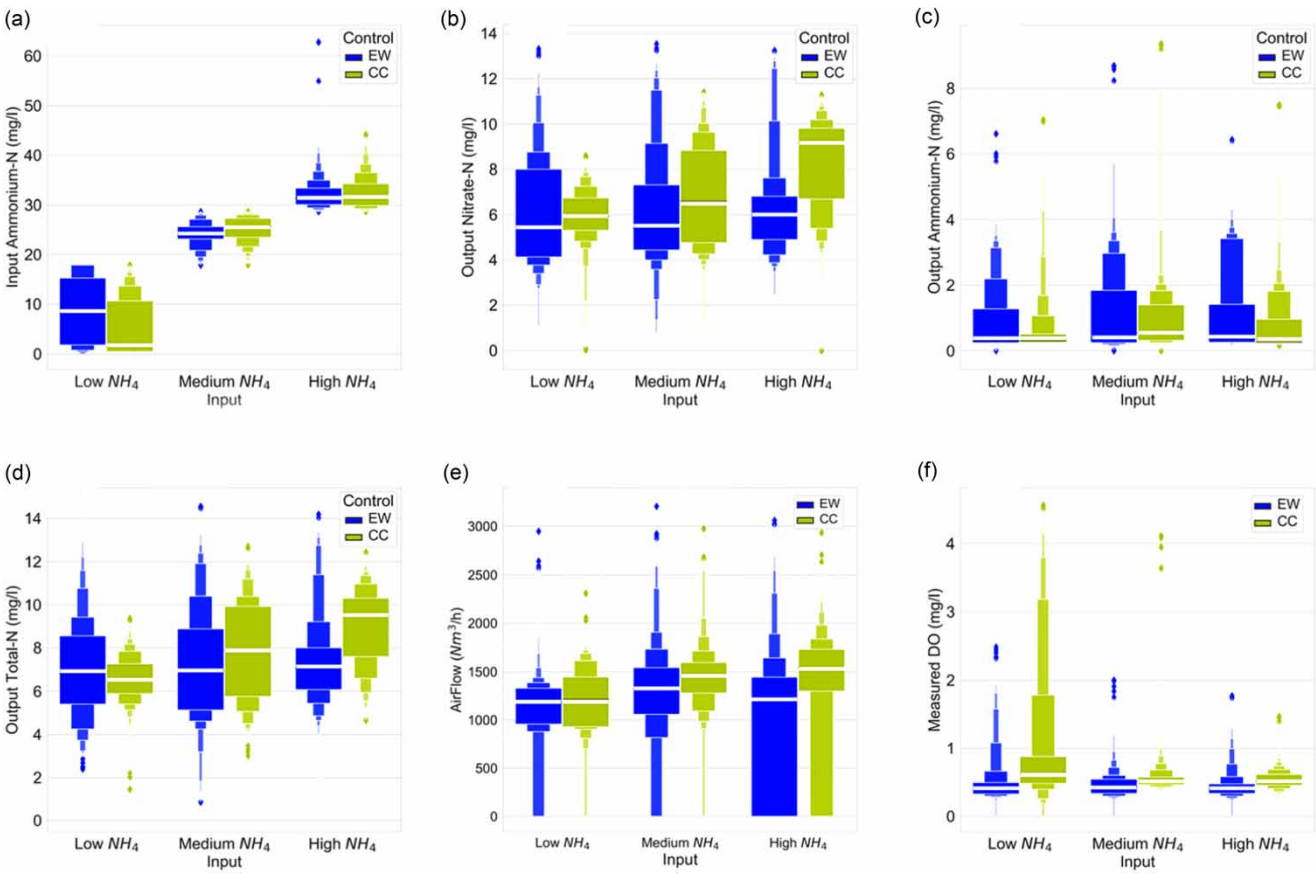

Figure 8 | Box plots of the controller performances over the period 10 June – 9 Sept. 2019. The band width represents the amount of data in the 5th, 25th, 50th, 75th, and 95th percentiles, while the mean value is represented by the white segment. (a) Distribution of input NH_4; (b) distribution of output NO_3; (c) distribution of output NH_4; (d) distribution of N_{tot}; (e) distribution of air flow; (f) distribution of DO.

From the values of Table 2, the percentage improvements of the EW controller are computed in Table 3, assessing the improvement of EW over CC.

To better appreciate the differing behaviour of the two controllers over the test period of weekly switching, several box plots were produced, as shown in Figure 8. As noted, the NH_4 input ranges were about the same for both controllers (Figure 8(a)), and the thickness of the Low plot shows that the low loading was the most common situation. Conversely, Figure 8(b), 8(c), and 8(d) show that the effluent quality obtained by the EW controller was consistently lower than in the CC case, save for the output N_{tot} that was slightly higher in the Low input case, though this increase is hardly significant, and well within the limit. For the air flow, which is strictly related to the energy consumption, Figure 8(e) shows that under the EW controller management the aeration was consistently lower than in the CC case. Further, the wider box of the Low percentiles in the High input case indicates a net energy saving for the EW controller. This is also reflected in the lower DO values shown in Figure 8(f), particularly evident in the Low input case, when the CC produced a higher DO, with the risk of adversely affecting the sedimentation characteristics of the sludge.

CONCLUSIONS

This paper has described the design and field testing of the EW MPC based on neuro-fuzzy networks and heuristic search. Its main asset is the ability to predict the N_{tot} peaks sufficiently in advance (α >30 min) to adapt the air low and secure safe effluent standards while saving energy.

During the initial test, the two controllers (EW and CC) were alternatively engaged as shown in Figure 6. The flexibility of the EW controller is further demonstrated by comparing the average relative weights of the cost function Equations (2) and (3) in two periods with differing treatment requirements, as demonstrated in Figure 7.

Further tests obtained by alternating the two controllers on a weekly basis have confirmed the improved reliability of the EW controller in achieving a better effluent quality while conserving energy, particularly by decreasing the air flow during the low load periods, but also by limiting the oxidation during high load peaks, provided that the nutrients limit is never reached. In all cases, the effluent is kept well within the regulatory limit. This aspect is demonstrated in statistical terms in Figure 8, where the EW controller compares favourably to the previous scheme, being able to consistently shift the percentile plots towards lower values of each output indicator and of the air flow.

The system is presently in operation at the previously mentioned plant, where its testing against the conventional controller continues.

ACKNOWLEDGEMENT

The authors gratefully acknowledge the collaboration of HERA SpA for supporting this research and for consenting to the present publication.

DATA AVAILABILITY STATEMENT

All relevant data are included in the paper or its Supplementary Information.

REFERENCES

Babuska, R. 1998 *Fuzzy Modeling for Control*. Kluver Academic Publ., Boston, MA, pp. 260.

Bartoletti, N., Casagli, F., Marsili-Libelli, S., Nardi, A. & Palandri, L. 2018 Data-driven rainfall/runoff modelling based on a neuro-fuzzy inference system. *Environmental Modelling and Software* **106**, 35–47.

Borrelli, F., Bemporad, A. & Morari, M. 2017 *Predictive Control for Linear and Hybrid Systems*. Cambridge University Press, Cambridge, UK, pp. 440.

Castillo, A., Cheali, P., Gómez, V., Comas, J., Poch, M. & Sin, G. 2016 An integrated knowledge-based and optimization tool for the sustainable selection of wastewater treatment process concepts. *Environmental Modelling and Software* **84**, 177–192.

Corominas, L., Garrido-Baserba, M., Villez, K., Olsson, G., Cortés, U. & Poch, M. 2018 Transforming data into knowledge for improved wastewater treatment operation: a critical review of techniques. *Environmental Modelling and Software* **106**, 89–103.

Dainotto, A., Barni, G., Giaccherini, F., Magnolfi, V., Marsili-Libelli, S. & Simonetti, I. 2012 A multilevel coordinated control strategy for energy conservation in wastewater treatment plants. In: *PID '12, IFAC Conference on Advances in PID Control, Brescia*, WePS10.

Dürrenmatt, D. J. & Gujer, W. 2011 Data-driven modeling approaches to support wastewater treatment plant operation. *Environmental Modelling & Software* **30**, 47–56.

Fernandez de Canete, J., Del Saz-Orozco, P., Baratti, R., Mulas, M., Ruano, A. & Garcia-Cerezo, A. 2016 Soft-sensing estimation of plant effluent concentrations in a biological wastewater treatment plant using an optimal neural network. *Expert Systems with Applications* **63**, 8–19.

Foscoliano, C., Del Vigo, S., Mulas, M. & Tronci, S. 2016 Predictive control of an activated sludge process for long term operation. *Chemical Engineering Journal* **304**, 1031–1044.

Francisco, M., Skogestad, S. & Vega, P. 2015 Model predictive control for the self-optimized operation in wastewater treatment plants: Analysis of dynamic issues. *Computers and Chemical Engineering* **82**, 259–272.

Giusti, E. & Marsili-Libelli, S. 2010 Fuzzy modelling of the composting process. *Environmental Modelling & Software* **25**, 641–647.

Giusti, E. & Marsili-Libelli, S. 2015 A fuzzy decision support system for irrigation and water conservation in agriculture. *Environmental Modelling & Software* **63**, 73–86.

Goldar, A., Revollar, S. R., Lamanna, R. & Vega, P. 2016 Neural NLMPC schemes for the control of the activated sludge process. In: IFAC-PapersOnLine, pp. 913–918.

Goldberg, D. E. 1989 *Genetic Algorithms in Search, Optimization, and Machine Learning*. Addison Wesley, Reading, MA, USA, pp. 412.

Hagan, M. T., Demuth, H. B. & Beale, M. 1996 *Neural Network Design*. PWS Publ. Co., Boston, MA, USA, pp. 637.

Haimi, H., Mulas, M., Corona, F. & Vahala, R. 2013 Data-derived soft-sensors for biological wastewater treatment plants: an overview. *Environmental Modelling & Software* **47**, 88–107.

Haimi, H., Mulas, M., Corona, F., Marsili-Libelli, S., Lindell, P., Heinonen, M. & Vahala, R. 2016 Adaptive data-derived anomaly detection in the activated sludge process of a large-scale wastewater treatment plant. *Engineering Applications of Artificial Intelligence* **52**, 65–80.

Han, H. & Qiao, J. 2014 Nonlinear model-predictive control for industrial processes: an application to wastewater treatment process. *IEEE Transactions on Industrial Electronics* **61**, 1970–1982.

Holenda, B., Domokos, E., Rédey, Á. & Fazakas, J. 2008 Dissolved oxygen control of the activated sludge wastewater treatment process using model predictive control. *Computers and Chemical Engineering* **32**, 1270–1278.

Holland, J. H. 1998 *Adaptation in Natural and Artificial Systems: An Introductory Analysis With Applications to Biology, Control, and Artificial Intelligence*. MIT Press, Cambridge, MA, USA, pp. 232.

Hong, Y. S. & Bhamidimarri, R. 2003 Evolutionary self-organising modelling of a municipal wastewater treatment plant. *Water Research* **37**, 1199–1212.

Iglesias, A., Dafonte, C., Arcay, B. & Cotos, J. M. 2007 Integration of remote sensing techniques and connectionist models for decision support in fishing catches. *Environmental Modelling & Software* **22**, 862–870.

Jang, J. R. 1993 ANFIS: adaptive-network-based fuzzy inference system. *IEEE Trans. on Systems, Man, and Cibernetics* **23**, 665–685.

Judson, P. 2019 *Knowledge-based Expert Systems in Chemistry: Artificial Intelligence in Decision Making*. Royal Society of Chemistry, London, UK, pp. 284.

Kosko, B. 1992 Neural networks and fuzzy systems. Prentice-Hall, London, pp. 449.

Mannina, G., Rebouças, T. F., Cosenza, A., Sànchez-Marrè, M. & Gibert, K. 2019 Decision support systems (DSS) for wastewater treatment plants – a review of the state of the art. *Bioresource Technology* **290**, 121814.

Marsili-Libelli, S. 2016 *Environmental Systems Analysis with MATLAB*. CRC Press, Boca Raton, FL, USA, pp. 546.

Marsili-Libelli, S. & Giunti, L. 2002 Fuzzy predictive control for nitrogen removal in biological wastewater treatment. *Water Science and Technology* **45**, 37–44.

Mulas, M., Tronci, S., Corona, F., Haimi, H., Lindell, P., Heinonen, M., Vahala, R. & Baratti, R. 2013 An application of predictive control to the Viikinmäki wastewater treatment plant. *IFAC Proceedings Volumes (IFAC-PapersOnline)* **12**, 18–23.

Mulas, M., Tronci, S., Corona, F., Haimi, H., Lindell, P., Heinonen, M., Vahala, R. & Baratti, R. 2015 Predictive control of an activated sludge process: an application to the Viikinmaki wastewater treatment plant. *Journal of Process Control* **35**, 89–100.

Nikolopoulos, C. 2019 *Expert Systems: Introduction to First and Second Generation and Hybrid Knowledge Based Systems*. Routledge, New York, USA, pp. 352.

O'Brien, M., Mack, J., Lennox, B., Lovett, D. & Wall, A. 2011 Model predictive control of an activated sludge process: a case study. *Control Engineering Practice* **19**, 54–61.

Qiao, J. F., Hou, Y., Zhang, L. & Han, H. G. 2018 Adaptive fuzzy neural network control of wastewater treatment process with multiobjective operation. *Neurocomputing* **275**, 383–393.

Rawlings, J. B., Mayne, D. Q. & Diehl, M. M. 2017 *Model Predictive Control: Theory, Computation, and Design*. Nob Hill Publ., London, UK, pp. 623.

Snip, L. J. P., Boiocchi, R., Flores-Alsina, X., Jeppsson, U. & Gernaey, K. V. 2014 Challenges encountered when expanding activated sludge models: a case study based on N_2O production. *Water Science and Technology* **70**, 1251–1260.

Stare, A., Vrečko, D., Hvala, N. & Strmčnik, S. 2007 Comparison of control strategies for nitrogen removal in an activated sludge process in terms of operating costs: a simulation study. *Water Research* **41**, 2004–2014.

Takagi, T. & Sugeno, M. 1985 Fuzzy identification of systems and its applications to modeling and control. *IEEE Trans. on Systems, Man, and Cibernetics* **15**, 116–132.

Tay, J. & Zhang, X. 1999 Neural fuzzy modeling of anaerobic biological wastewater treatment systems. *ASCE Journal of Environmental Engineering* **125**, 1149–1159.

Tay, J. H. & Zhang, X. 2000 A fast predicting neural fuzzy model for high-rate anaerobic wastewater treatment system. *Water Research* **34**, 2849–2860.

Torregrossa, D., Hernández-Sancho, F., Hansen, J., Cornelissen, A., Popov, T. & Schutz, G. 2018 Energy saving in wastewater treatment plants: a plant-generic cooperative decision support system. *Journal of Cleaner Production* **167**, 601–609.

Wu, W., Dandy, G. C. & Maier, H. R. 2014 Protocol for developing ANN models and its application to the assessment of the quality of the ANN model development process in drinking water quality modelling. *Environmental Modelling and Software* **54**, 108–127.

Yager, R. R. & Zadeh, L. A. 1994 *Fuzzy Sets, Neural Networks, and Soft Computing*. Van Nostrand Reinhold, New York, USA, pp. 440.

Zhao, L., Dai, T., Qiao, Z., Sun, P., Hao, J. & Yang, Y. 2020 Application of artificial intelligence to wastewater treatment: a bibliometric analysis and systematic review of technology, economy, management, and wastewater reuse. *Process Safety and Environmental Protection* **133**, 169–182.

First received 5 February 2020; accepted in revised form 6 June 2020. Available online 19 June 2020